



Numerical Analysis of the Dead-Band Clearance Effect on the Vibrations of a Vertical Rotor

Lassad Amami, Mihai Arghir^(✉), and Pascal Jolly

Institut PPRIME, UPR CNRS 3346, Université de Poitiers, ISAE ENSMA,
11 bd. Pierre et Marie Curie, BP 30179,
86962 Futuroscope Chasseneuil Cedex, France
mihai.arghir@univ-poitiers.fr

Abstract. The present work tackles the dead band clearance problem of rotors guided by ball or roller bearings. There are situations when the rotor can be only temporary in contact with the casing. The closed-loose nature of the rotor-stator contact leads to a non-linear rotordynamic response. A test rig dedicated to the experimental analysis of this problem was presented in a previous paper [8]. The test rig is based on a vertical rotor guided by ball bearings and lifted by an aerostatic thrust bearing. The ball bearings are mounted with three different radial clearances: “small”, “medium” and “large”. The results for the low and mild radial clearances showed a linear behavior of the rotor characterized by synchronous responses with forward or backward whirls. A non-linear signature of the rotor was obtained for the large radial clearance with sub-synchronous bifurcations and internal resonances. The present paper presents the numerical analysis of the same rotor and is intended to reproduce the experimental results. The rotor was modeled with Timoshenko beam elements. Full non-linear calculations were performed by simulating a constant acceleration of the rotor from zero to 400 Hz in 50 s. Calculations showed that the value of the dead-band clearance is a capital parameter for triggering non-linear responses of the rotor.

Keywords: Rotordynamics · Dead-band clearance problem

1 Introduction

Ball and roller bearings guiding rotors are generally mounted with no radial clearance between the outer ring and the casing of the machine. However, there are situations when a small radial clearance is present. Therefore, when operating, the rotor may be only temporary in contact with the casing. The gap between the rotor and the casing might be closed or loose. This closed-loose nature of the rotor-stator contact leads to a non-linear rotordynamic response known as the dead-band clearance (DBC) problem. The literature shows that when present in a rotating machinery, a dead-band clearance triggers a typical non-linear response of the rotor.

A non-linear analytic model for investigating the influence of the radial clearance was developed by Yamamoto early in 1959 [1]. It was shown that an increase of the ratio between the radial clearance and the unbalance eccentricity lead to a decrease of

the rotor critical speed. Following this results, the DBC is associated with a modification of the critical speed. Childs performed a similar theoretical analysis [2]. His results confirmed Yamamoto's findings but also showed that the radial clearance between the outer ring of the ball bearings and the casing is the source of sub-synchronous vibrations. Moreover, Childs underlines that the amplitudes of sub-synchronous vibrations increase with increasing unbalance while the amplitudes of synchronous components decrease. Other theoretical analyses [3, 4] confirmed the previous findings, namely that the increase of the DBC decreases the critical speeds and the vibration amplitudes at critical speeds.

In 1993 Lin [5] presents a simple experimental test rig based on a slender rotor with a disk at its mid-length and guided by two ball bearings at its ends. The ball bearing situated at the non-drive end had an adjustable DBC. Sub-synchronous vibrations due to the DBC were measured when the rotation speed was close to twice the first critical frequency. The frequency of the sub-synchronous vibrations was constant and equal to the first critical frequency. The sub-synchronous vibrations were present only near the rotation speed equal to twice the first critical and disappeared once the rotation speed increases. Lin [5] considers that the sub-synchronous component is not a self-sustained vibration but a benign regime triggered by the DBC. This observation was also underlined in a slightly different context [6, 7].

A paper recently presented by Amami et al. [8] was focused on the experimental analysis of the DBC problem in a vertically mounted, complex rotor. The test rig components were designed for three values of the DBC (small, medium and large) but, due to manufacturing errors, the experiments enlightened a somewhat different situation. The results for the small and medium radial clearances showed a linear behavior of the rotor characterized by synchronous responses with forward or backward whirls. A non-linear signature of the rotor was obtained for the large radial clearance with sub-synchronous bifurcations and internal resonances.

The present paper presents the numerical analysis of the rotor tested in [8] and is intended to reproduce the experimental results. The rotor was modeled with Timoshenko beam elements and contacts between the rotor and the casing were modeled with a contact stiffness. Full non-linear calculations were performed by simulating a constant acceleration of the rotor from zero to 400 Hz in 50 s.

Calculations showed that the value of the dead-band clearance is a capital parameter for triggering non-linear responses of the rotor. The numerical results for zero clearance and anisotropic support stiffness reproduced qualitatively the linear responses evidenced by experimental findings for small and medium DBC. High amplitude, sub synchronous vibrations were obtained for non-zero values of the clearance.

2 Summary of the Experimental Results

2.1 Description of the Test Rig

Figure 1 depicts the rotor and its vertical installation in the test rig. The rotor has three disks. It is guided by two pair of ball bearings, by two aerostatic bearings, is supported

at its bottom end by an aerostatic thrust bearing and is entrained at its upper end by an impulse (Pelton) turbine. The aerostatic bearings replace the annular straight seals normally present in the rotating machine. They are strongly pressurized and they represent the only source of radial damping of the rotor. The thrust bearing lifts the rotor and enables its rotation with a minimal torque. It is mounted on a wire mesh damper for minimizing the amplitudes of any axial vibration that could interfere.

The ball bearings are mounted by pairs and are axially preloaded by a wave spring. They are mounted with a radial clearance between the outer rings and the casing of the test rig. The variation of this clearance is obtained by manufacturing the casing parts of the test rig with different inner diameters. Each disk of the rotor is provided with two inductive, orthogonally mounted displacements probes. An optical probe and a mark on the top disk measure the rotation speed and the reference phase.

2.2 Experimental Results

Experimental results were obtained in [8] with three different radial clearances between the outer rings and the casing of the test rig. These clearances are designated as “small”, “medium” and “large”. Tests were performed by entraining the rotor up to 400 Hz followed by a free coast down.

Figure 2 depicts the full spectrum plots recorded on the upper (# 1) and on the lower disk (# 3) for the “small” DBC during acceleration from 0 to 400 Hz. The vibration amplitudes of the middle disk (# 2) are much lower because it is mounted very close to the node of the rigid conical mode. Therefore, for brevity, the results obtained for this disk are not presented.

The presence of only the synchronous component on Fig. 2 indicates a linear response of the rotor. This means that the outer ring of the ball bearings is continuously in contact with the casing. The explanation of this result is the fact that the “small” DBC was eliminated by the manufacturing errors.

The full spectrum diagrams show distinct zones of forward and backward whirls. The switch from forward to backward whirl and again to forward whirl occurs when the direct stiffness of the support is anisotropic. This means that the contact conditions of the outer rings of the ball bearings with the casing are anisotropic.

The results obtained with the “medium” DBC, twice larger than the previous one are depicted in Fig. 3 and show the same linear response. However, the backward precession is present on a shorter interval and for lower values of the rotation frequency. This means the contact stiffness decreased following the increase of the DBC from “small” to “medium”.

The results obtained with the “large” DBC, three times larger than the “small” DBC are depicted in Fig. 4. A net clearance between the outer rings of all ball bearings and the casing is now obtained. The diagrams show a clear non-linear response. A first critical frequency close to 140 Hz following X and Y is detected. This critical frequency was close to 230 Hz for the “small” DBC, decreased to 160 Hz for the “medium” DBC and was identified only following the X direction. A second critical speed following the Y direction is visible at 220 Hz. This critical speed was identified close to 320 Hz for the “small” DBC and decreases to 225 Hz for the “medium” DBC.

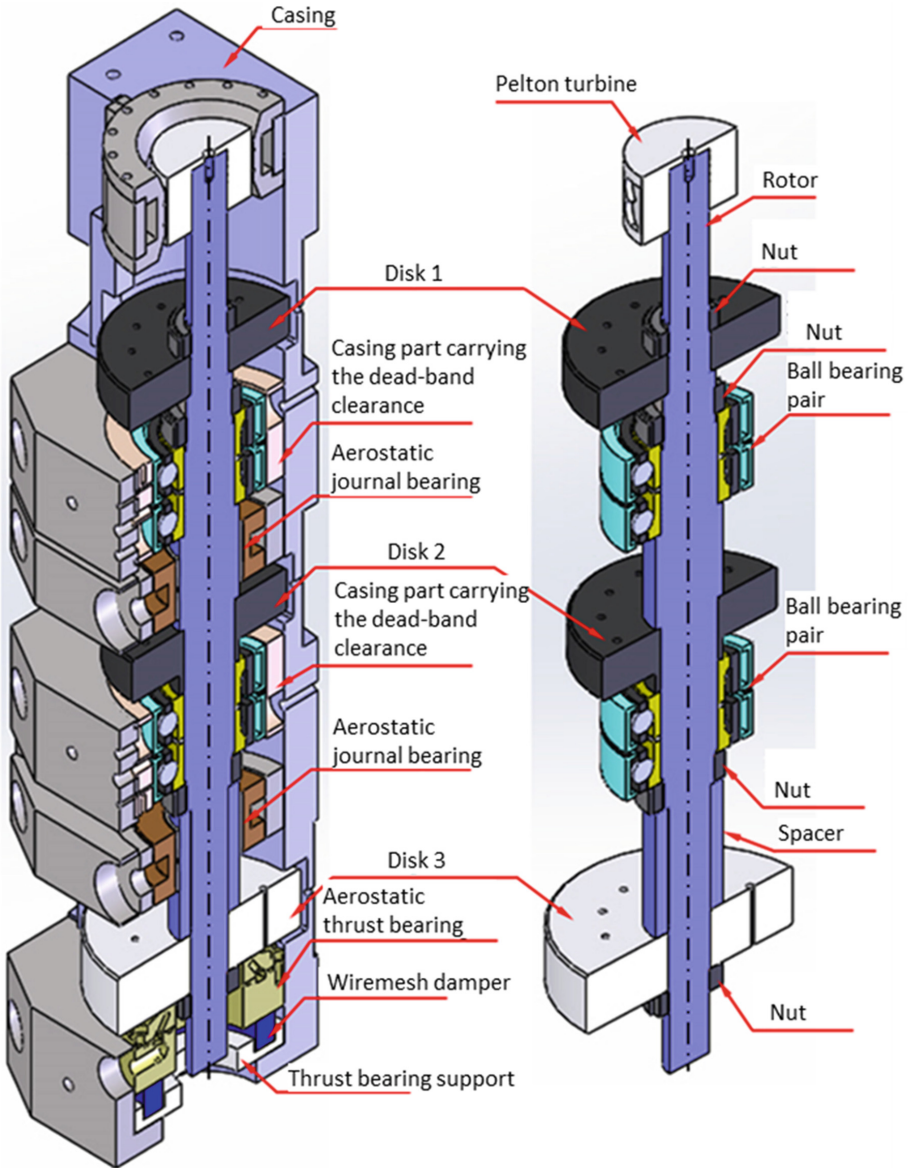


Fig. 1. The rotor and its installation in the test rig [8]

The critical speeds identified for the “large” DBC are systematically lower than those identified for the “small” and “medium” DBC. For rotation frequencies higher than 220 Hz, the response is clearly non-linear, the results showing a bifurcation followed by sub-synchronous vibrations. A clear sub-synchronous component detaches at a rotation frequency close to 220 Hz. This component becomes rapidly vertical and of large amplitude, its frequency being fixed at a constant value comprised between 130 and 140 Hz and corresponding to the first critical speed.

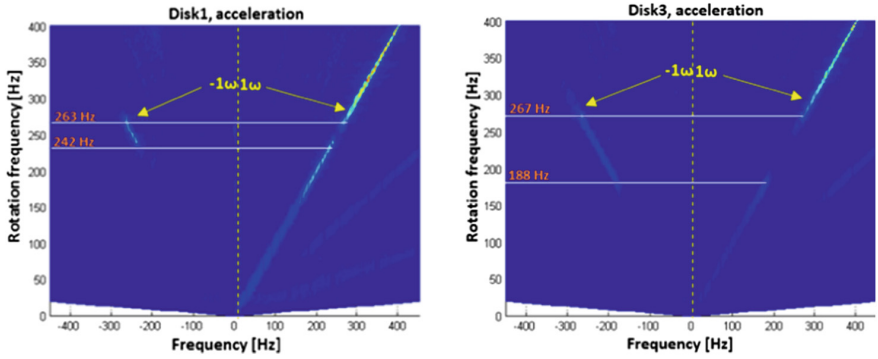


Fig. 2. Full-spectrum plot for the «small» DBC [8]

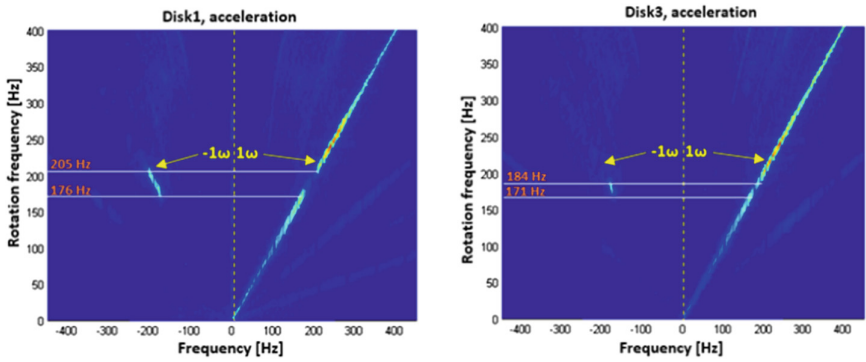


Fig. 3. Full-spectrum plot for the «medium» DBC [8]

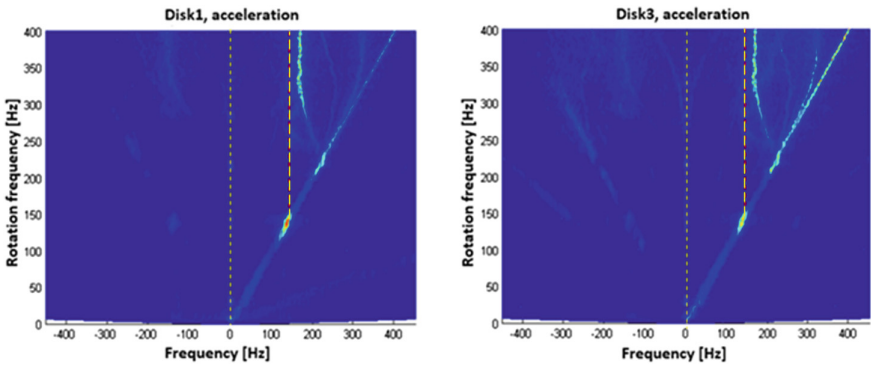


Fig. 4. Full-spectrum plot for the «large» DBC [8]

3 Rotor Model

The rotor was modeled with Timoshenko beam elements. The ball bearings and the contacts were modeled with a contact stiffness as further indicated in Sects. 4.1 and 4.2.

Rayleigh damping was added to the rotor model after experimental tests. As indicated in Fig. 5a, impacts were applied at one end of the suspended rotor and acceleration responses were measured on the second disk. The frequency response is depicted in Fig. 5b. Modal damping was identified by using the half power method and the approximation of Rayleigh damping is depicted in Fig. 6.

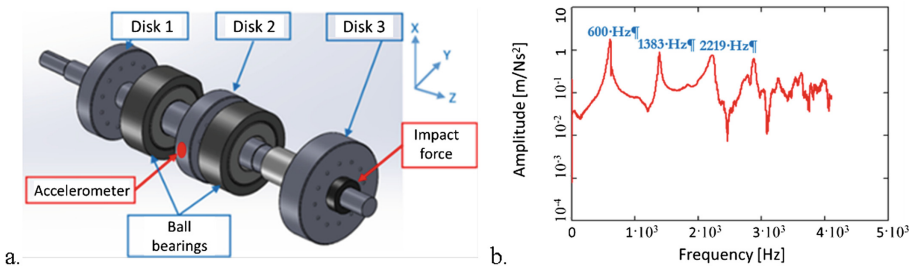


Fig. 5. Frequency response of the suspended (free-free) rotor

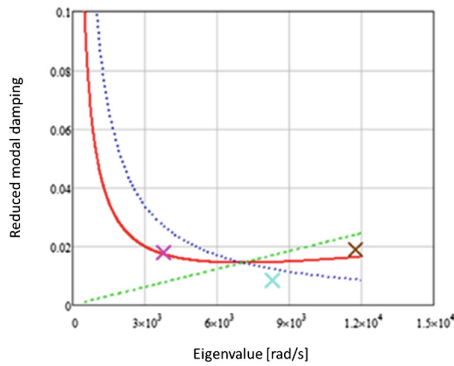


Fig. 6. Approximation of the Rayleigh damping

4 Numerical Analysis

The numerical simulation of this DBC problem is a quite difficult task due to the large number of unknown parameters that must be selected and triggered. The simulation is performed in two steps: first for the “small” and “medium” DBC where, due to manufacturing errors, the non-linear response was not present and then for the “large” DBC.

4.1 Results for the “Small” and “Medium” DBC

As mentioned, for the “small” and “medium” DBC configurations, the experimental results showed a linear response of the rotor. This was a clear indication that the outer rings of the ball bearings were constantly in contact with the casing and no DBC was present. However, the contact stiffness proved to be anisotropic because the results enlightened two conical modes, following X and Y and a shift from forward to backward and again to forward whirl. After trials, a value of $2.5 \cdot 10^6$ N/m was adopted for the X stiffness of each ball bearing and 10^7 N/m for the Y stiffness. These parameters were further refined by adopting a $3.5 \cdot 10^6$ N/m value for the X stiffness of the lower pair of ball bearings depicted in Fig. 1. The two aerostatic bearings were considered to have a direct stiffness of $2.6 \cdot 10^6$ N/m; their cross coupling stiffness and direct damping was discarded. Full non-linear calculations were performed by simulating a constant acceleration of the rotor from zero to 400 Hz in 50 s. Estimating the unbalance amount is also difficult. After trials and comparisons with the experimental results, two 1.5 g mm unbalances were added at the ends of the rotor with a 120° phase difference.

The results are depicted in Figs. 7 and 8 for disks 1 and 3.

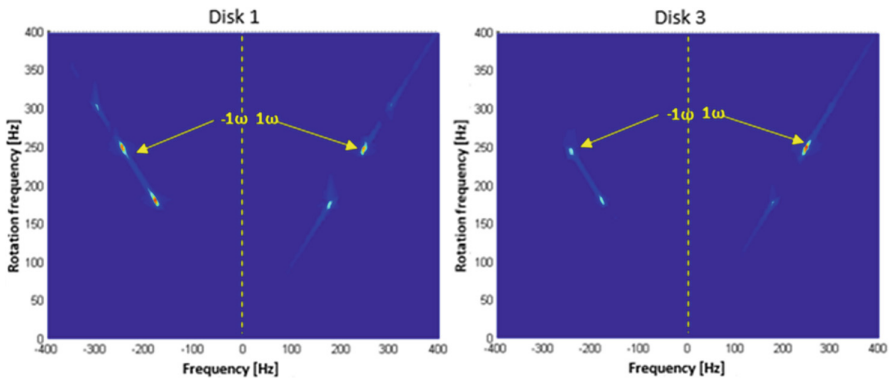


Fig. 7. Numerical full-spectrum plots obtained for the rotor model without DBC

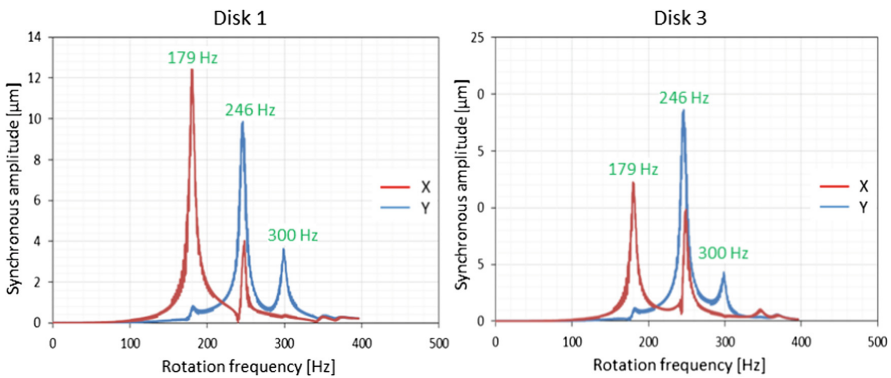


Fig. 8. Synchronous amplitudes obtained for the rotor model without DBC

The full-spectrum diagrams depicted in Fig. 7 clearly show the backward whirl. The disks 1 and 3 show a forward whirl from 0 to 179 Hz, a backward whirl between 179 and 246 Hz and again a forward whirl up to 400 Hz. The synchronous amplitudes of the disks depicted in Fig. 8 enable also to identify the X and Y modes. These plots are close to the experimental results obtained for the “small” DBC depicted in Fig. 2.

4.2 Results for the “Large” DBC

The experimental results obtained for the “large” DBC showed a different, non-linear signature. The loose contact between the outer rings of the ball bearings and the casing was modeled by imposing a radial clearance and a contact stiffness of 10^{12} N/m. If the radial displacement of the corresponding discretization node is lower than the radial clearance, then no force is imposed, otherwise the contact stiffness becomes active. No friction arising from contact was considered. This is a realistic assumption because the outer rings of the ball bearings can freely rotate. The value of the radial clearance was the same in X and Y directions and for all ball bearings. The values of the other parameters were the same as for the “small” and “medium” DBC and calculations were again performed by simulating a constant acceleration from zero to 400 Hz in 50 s.

Figure 9 depicts the results obtained with values of the DBC from 5 to 20 μm . Results obtained with a DBC of 5 μm show two synchronous amplitude peaks at 125 and 170 Hz and two corresponding sub-synchronous components starting with 300 Hz. A backward whirl regime is also present in the response of disk 3. The results are similar for a DBC of 10 μm but a chaotic regime is present for rotation frequencies comprised between 170 and 280 Hz. Moreover, the backward whirl regime vanishes. Following the increase of the DBC at 15 μm , the 170 Hz synchronous amplitude peak of disk 1 disappears with but remains present on disk 3. The chaotic regime is still present but on a lesser extent. The chaotic regime disappears with the further increase of the DBC at 20 μm . Two amplitude peaks are identified on disk 3 at 125 and 190 Hz and a single peak on disk 1 at 125 Hz. The chaotic regime is absent and sub-synchronous vibrations of constant frequency are triggered at 125 and 190 Hz. In all cases, the amplitudes of the sub-synchronous vibrations are very large if not dominant.

A 12 μm value of the DBC gave the closest agreement with the experimental results depicted in Fig. 4. The theoretical full spectrum diagrams of the amplitudes are depicted in Fig. 10. The diagrams show no backward whirl. A first amplitude peak is identified at 120 Hz for both disks; a second peak appears at 170 Hz but only for the disk 3. These values are lower than the frequencies of the corresponding modes underlined for the “small” and “medium” DBC. A sub synchronous component is visible on disk 1 for rotation frequencies larger than 120 Hz followed by a quasi-periodic regime after 170 Hz. Two sub synchronous components appear for disk 3, triggered at rotation frequencies of 120 and 170 Hz. Figure 11 depicts the synchronously filtered amplitudes. It should be underlined that for rotation frequencies larger than 120 and 170 Hz, when the regime is highly non-linear, a large percentage of energy is carried by the sub synchronous components (i.e. their amplitudes are larger than the synchronous ones).

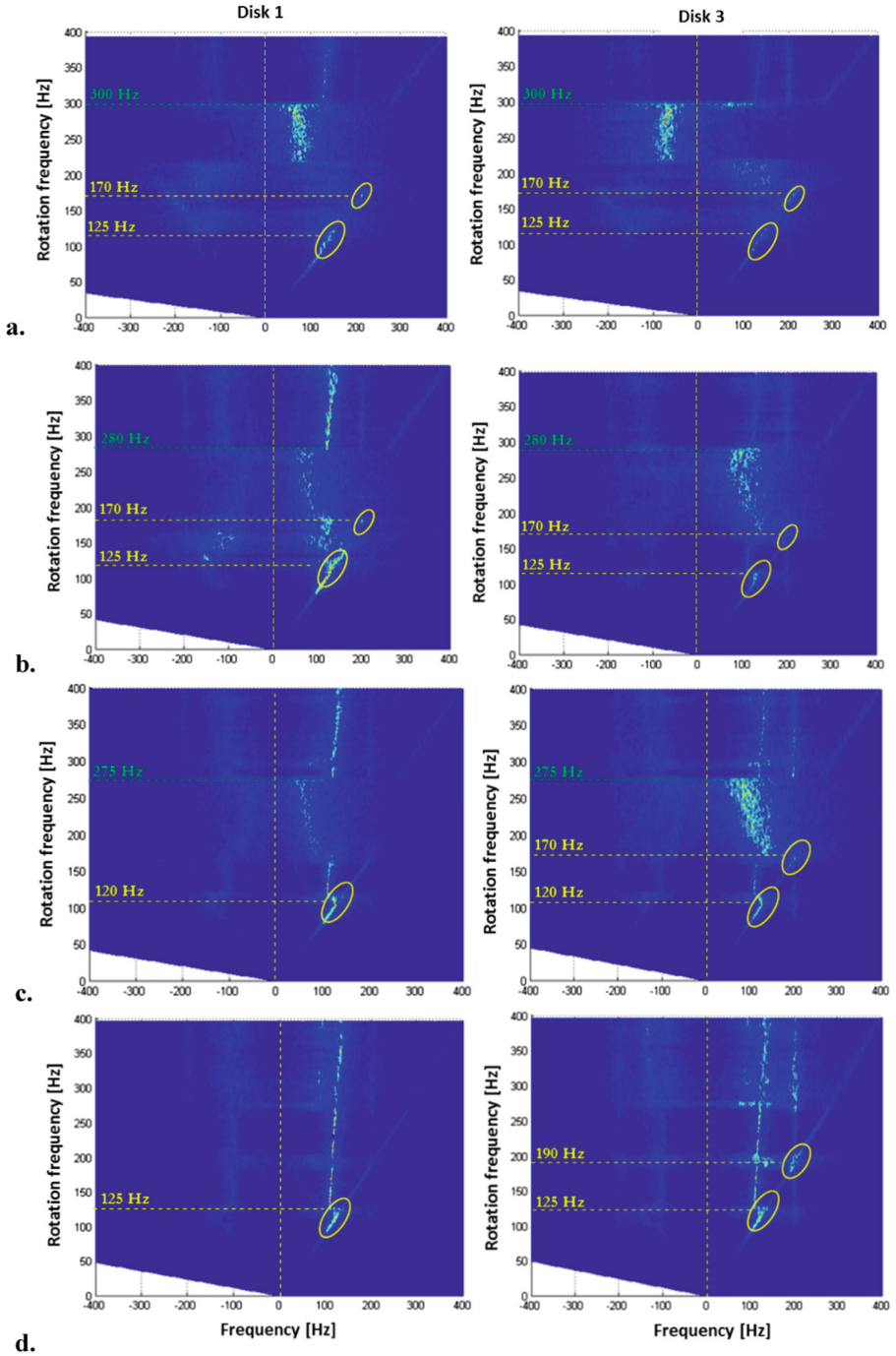


Fig. 9. Parametric analysis of the impact of the DBC (a. 5 μm , b. 10 μm , c. 15 μm , d. 20 μm)

The comparison between Figs. 4 and 10 shows only a limited agreement. This is due to the large number of parameters that must be selected and carefully triggered. A systematic parametric analysis including also the contact stiffness can be found in [9].

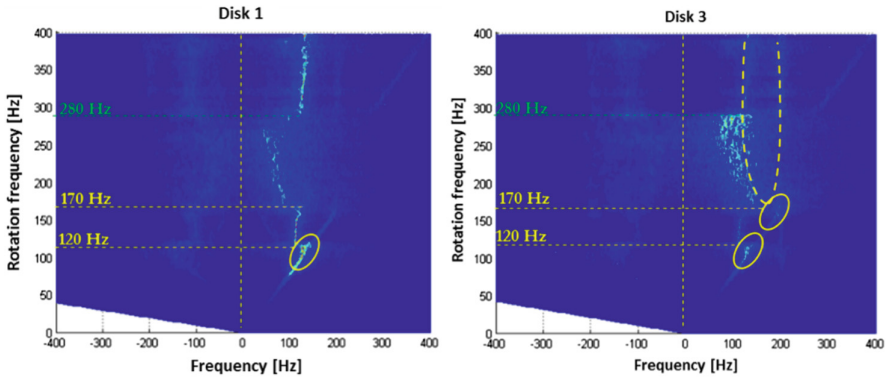


Fig. 10. Numerical full-spectrum plots obtained for the rotor model with a 12 μm DBC

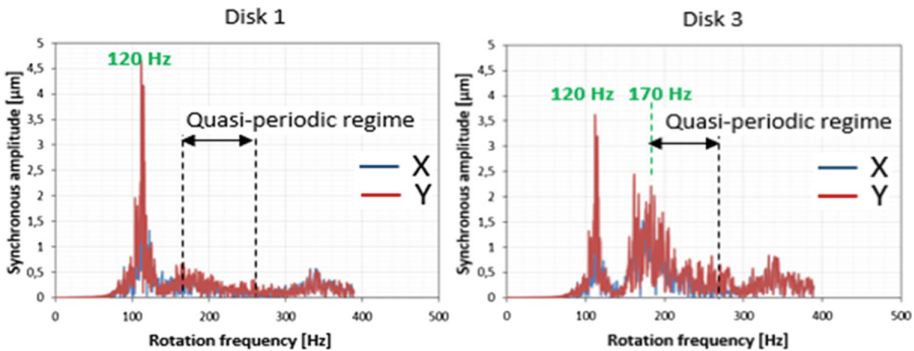


Fig. 11. Synchronous amplitudes obtained for the rotor model with a 12 μm DBC

5 Summary and Conclusions

The paper presents the impact of the DBC on the dynamic response of a complex rotor. Two pairs of ball bearings guided the vertically mounted rotor. Numerical results were obtained by performing a full non-linear analysis with a traditional rotordynamic model. The analysis was performed for a case with no DBC but with anisotropic stiffness and for cases with DBC comprised between 5 and 20 μm . The results show that the value of the DBC is a capital parameter: high amplitude, sub synchronous vibrations or chaotic regimes can be triggered depending on the value of this clearance.

It was found that the results obtained with a DBC of 12 μm agree qualitatively with the test rig measurements for the “large” radial clearance. They also confirm the

theoretical predictions from the references discussed in the introduction part of the paper, namely, the presence of the DBC lowers the critical frequencies and triggers a non-linear response with high amplitude sub-synchronous components. The numerical simulations also underline the multitude of parameters that must be introduced into a rotordynamic model for correctly simulating non-linear responses, the value of the dead-band clearance being of capital importance.

Acknowledgements. The authors are grateful to Centre National d'Etudes Spatiales and to Airbus Safran Launchers for supporting this work.

References

1. Yamamoto, T.: On Critical Speeds of a Shaft. *Memoirs of the Faculty of Engineering, Nagogo University*, vol. 6, no. 12 (1959)
2. Childs, D.W.: Fractional frequency rotor motion due to non-symmetric clearance effects. *J. Eng. Power* **104**, 533–541 (1982)
3. Gogging, D.G., Darden, J.M.: Limiting critical speed response on the SSME alternate high pressure fuel turbopump (ATD HPFTP^o with bearing deadband clearance). 28th Joint Propulsion Conference and Exhibit, Nashville (1992)
4. Butner, M.F., Murphy, B.T., Akian, R.A.: The influence of mounting compliance and operating conditions on the radial stiffness of ball bearing: analytic and test results. *ASME, DE-Vol. 35, Rotating Machinery and Vehicle Dynamics*, pp. 155–162 (1991)
5. Lin, Y.-Q.: Rotor instability induced by deadband clearance in bearing supports. Ph.D. thesis, Texas A&M University, USA (1993)
6. Rahul, K.: Diagnostics of subsynchronous vibrations in rotating machinery - methodology to identify potential instability. MS thesis, Texas A&M University, USA (2005)
7. Rajagopalan, V.N.: Diagnostic subsynchronous vibration turbomachinery - stable or unstable. MS Thesis, Texas A&M University, USA (2007)
8. Amami, L., Arghir, M., Jolly, P.: Experimental analyses of the dead-band clearance effect on the vibrations of a vertical rotor, *IMEchE VIRM 4*, Manchester, UK (2016)
9. Amami, L.: Analyse expérimentale de la réponse dynamique d'un rotor vertical guide par des roulements avec jeu. Thèse de doctorat, Université de Poitiers, France (2016)